

Experiments on Rock-Bit Interaction during a Combined Thermo-Mechanical Drilling Method

Edoardo Rossi^{1,2}, Michael A. Kant¹, Oskar Borkeloh¹, Martin O. Saar² and Philipp Rudolf von Rohr¹

¹ETH Zürich, Transport Processes and Reactions Laboratory, Institute of Process Engineering, Sonneggstr. 3, 8092 Zürich, Switzerland

²ETH Zürich, Geothermal Energy and Geofluids, Institute of Geophysics, Sonneggstr. 5, 8092 Zürich, Switzerland

rossie@ethz.ch

Keywords: Alternative Drilling Methods, Enhanced Drilling, Hard Rock Drilling Rock Abrasivity, Rock-Bit Interaction, Thermal Treatments

ABSTRACT

The development of deep geothermal systems to boost global electricity production relies on finding cost-effective solutions to enhance the drilling performance in hard rock formations. Conventional drilling methods, based on mechanical removal of the rock material, are characterized by high drill bit wear rates and low rates of penetration (ROP) in hard rocks, resulting in high drilling costs, which account for more than 60% of the overall costs for a geothermal project. Therefore, alternative drilling technologies are investigated worldwide with the aim of improving the drilling capabilities and therewith enhancing the exploitation of deep geothermal resources. In this work, a promising drilling method, where conventional rotary drilling is thermally assisted by a flame-jet, is evaluated. Here, the thermal weakening of the rock material, performed by flame-jets, facilitates the subsequent mechanical removal performed by conventional cutters. The flame moves on the rock surface and thermally treats the material by inducing high thermal gradients and high temperatures, therewith reducing the mechanical properties of the rock. This would result in reduced forces on the drill bits, leading to lower bit wear rates and improved rates of penetration and therefore significantly decreasing the drilling costs, especially for deep-drilling projects.

In this work, the feasibility of the proposed drilling method is assessed by comparing the rock-bit interaction in sandstone and granite under baseline and thermally treated conditions. Rock abrasivity, tool penetration and cutting forces are investigated to quantify the rock-bit interaction in granite and sandstone under baseline conditions and after the thermal treatment. The results highlights the dominant mechanisms regulating the rock removal. The removal performance of the tool in the granite material are found to be greatly enhanced by the thermal treatment both in terms of volume removed from the sample and worn volume at the tool's tip. On the other hand, the sandstone material, after a thermal treatment, yields significantly lower wearing of the cutting tool. Thus, this results allow to draw important conclusions regarding the achievable drilling performances during the combined thermo-mechanical drilling method towards its application in the field.

1. INTRODUCTION

The high project costs are still a major factor hindering the worldwide exploitation of geothermal energy for electricity production. More than 60% of the total cost budget accounts for drilling and well completion operations [1, 2], following an exponential increase with depth, as shown by Tester et al. [3]. Indeed, in geothermal energy exploitation, deep wells in hard crystalline rocks have to be drilled. In this context, a reduction of the forces acting on the cutting tools must be achieved in order to improve drill bit life and attain higher rates of penetration [4]. A predominant figure influencing the drilling costs is the high rate of drill bit wearing when conventional drilling methods are used [5]. Therefore, in order to improve the effectiveness of drilling and reduce the related costs, alternative drilling methods, such as hammering [6], thermal spallation [7, 8], electro-pulse [9], plasma drilling [10], and hydraulic jetting processes [11] are investigated worldwide. An interesting technique to effectively drill hard rock materials is thermal spallation drilling [7, 8]. This method uses a hot fluid jet to induce high thermal stresses at the rock material's surface. This stress field is capable to cause the initiation of cracks in the material and to propagate pre-existing flaws, which then can combine to trigger the spallation phenomenon at the rock surface. This non-contact removal process is effective in hard rocks [7, 8, 12] where higher penetration rates are found, compared to conventional drilling. However, the thermal spallation mechanism cannot be sustained when soft materials or discontinuities in the rock mass are present [13, 14] and the drilling process is therewith inhibited.

A proposed approach to overcome the disadvantages of thermal spallation drilling and enhance the drilling performance is to combine thermal spallation drilling and conventional rotary drilling. This method, called combined thermo-mechanical drilling, uses a hot fluid jet to assist the material removal performed by conventional drilling cutters. In this manner, the thermal assistance can induce (i) the thermal spallation onset, when the material presents the required hard rock properties [8, 14] in order to achieve spallation, or (ii) the thermal weakening of the rock material [15], which is then exported by conventional drilling cutters. This method would allow a reduction of the forces exerted on the drill bits and lower drill bit wear rates, with correspondingly higher rates of penetration, compared to conventional drilling techniques.

In this work, we want to assess whether the thermal weakening of the material directly affects the drilling performances in terms of bit wearing and rate of penetration by evaluating the rock-bit interaction via laboratory experiments. The combined thermo-mechanical drilling method is experimentally modeled by thermally treating the rock material and studying the resulting interaction with a cutting tool under baseline material conditions and after the thermal treatment. The conclusions of this study will give insight into the performance improvements of the proposed combined thermo-mechanical drilling method for both a granite and a sandstone material.

2. A COMBINED THERMO-MECHANICAL DRILLING METHOD

In order to enhance drilling for deep geothermal resources, we propose a combined thermo-mechanical drilling method. This combination aims to intensify the conventional, rotary drilling process via a thermal assistance, provided, for instance, by flame-jets, which are located next to the mechanical drilling cutters. As shown in Figure 1, the drill head is composed of a combustion chamber, where the reactant fluids are ignited to generate the required heat power at the drill bit. Methane and oxygen can be used as combustion gases in order to provide a stable and high-power flame-jet. The combustion chamber is cooled down by high flowrates of drilling mud, which then exits at the end-face of the drill bit to circulate the cuttings and ensure the stability of the drilled wellbore. The hot exhausts exiting the combustion chamber are forced out of the drill bit through a series of nozzles by which flame-jets are generated. At the drill bit face, drilling mud circulates the produced cuttings whilst enabling the cooling of the rock surface, which has been thermally treated by the flame-jets. Drilling cutters are placed next to the flame nozzles around the drill bit in order to carry out the removal of the treated rock material. The flame-jets, although providing the thermal assistance to the drilling process by either weakening or spalling the rock material, they also introduce a significant amount of heat at the bit face, which might undermine the thermal stability of the cutter's material. Additionally, the flame-jets must endure the aqueous, drilling mud environment and transfer enough heat to the rock surface without major heat losses to the surrounding fluids [16-18]. Therefore, one approach to overcome these problems is to protect the flame-jets at the drill bit end-face using an air-shielding concept [19]. Therewith, a feeding line conveying compressed air from the surface to the drill bit is prescribed inside the drill string. This is then connected to apposite air channels, which are placed circularly around the flame nozzles at the drill bit end-face. This allows to radially constrain the heat transferred to the rock, and by this decreasing the heat dissipation towards the surrounding drilling mud and reducing the related entrainment issues of the hot fluid-jet.

In this work, we analyze the performance improvements of the proposed drilling method by comparing the rock-bit interaction of a granite and a sandstone rock materials under baseline and after an oven thermal treatment. The thermal assistance to conventional drilling is experimentally modeled by thermally treating the rock material at high temperature in an oven and testing the resulting removal characteristics of the cutting tool. The cooling performed by drilling mud is emulated by a water cooling process after the thermal treatment of the rock samples. In this manner, we finally evaluate the drilling performances of the combined thermo-mechanical drilling technique from the view of tool wear rate and rock exportation efficiency.

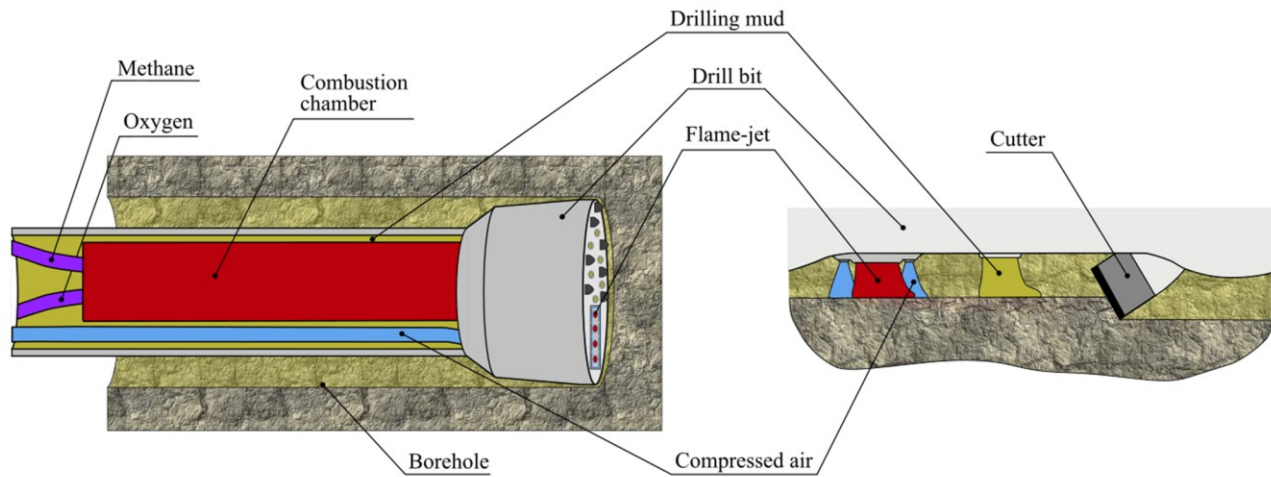


Figure 1: Combined thermo-mechanical drilling method with the main components of the drill head and the fluid streams.

3. EXPERIMENTAL METHODS

The rock-bit interaction permits an in-depth analysis of the tool capabilities in removing the rock material during drilling. In this work, we study different drilling parameters to evaluate the performances of the proposed combined thermo-mechanical drilling method. During the scraping process, performed by drilling cutters, abrasive removal of the material takes place at the rock surface. The instantaneous forces exerted on the cutter and the penetration of the cutting tool in the rock material regulate two fundamental parameters describing drilling performance: penetration rate and wear rate of the cutters. In the following work, a specific experimental setup is implemented which employs the Cerchar Abrasivity Index (CAI) to evaluate the material removal by a sharp cutter in both a hard granite and a sandstone material, during baseline conditions and after thermally treating the material at high temperature.

3.1 Materials

Samples used in this work are block samples of size 100mm x 80mm x 80mm. Therefore, the experiments are carried out on the smooth sample surface obtained by this procedure. In order to test different conditions, a granite and a sandstone material are selected for this work. Samples of Central Aare granite are taken from the Aare Massif in the Central Alps, Switzerland. This granite consists of 46% quartz, 31% feldspar, 20% plagioclase, 3% biotite, and minor amounts of chlorite. The grain size ranges from a few micrometers up to ≈ 4 mm [20]. The second material is a sandstone from Rorschach, Switzerland. It is composed of 35% quartz, 25% cements, 10% plagioclase, and 30% metamorphic, volcanic and sedimentary lithics. This sandstone possesses a fine and homogeneous grain size distribution ranging from $50\mu\text{m}$ to $200\mu\text{m}$ [15].

3.2 Testing setup: Rock-bit interaction

To monitor the rock removal during drilling, a quantitative evaluation of cutting forces, cutter's penetration, and wear rate of the cutting tool is required. This allows to conclude on the achievable performance improvements during the combined thermo-mechanical drilling technique.

Rock abrasiveness is one main factor influencing the bit lifetime in the tunneling, mining and drilling industry [21-24]. The Cerchar abrasivity index (CAI) is a commonly used methodology to describe rock abrasiveness and predict wear of cutting tools. It follows a simple testing layout, which was introduced by the Centre d'Etudes et Recherches des Charbonnages [25] and standardized by the ASTM [26]. In this work, a modified version of the West apparatus [27] is used. In order to measure the rock abrasivity following this test procedure, a scraping pin (90° tip angle) of given Rockwell Hardness ($HRC\ 55 \pm 1$) is employed to scratch the tested sample, under a specified normal load of 70N and at a fixed speed of 1mm/s. The wear flat at the tool's tip after the test is an indication of the rock abrasiveness and therefore the width of the wear flat is measured at the tip in units of 0.1mm and the number of units is reported as the CAI value. Although the standard CAI testing procedure prescribes a testing distance of 10mm, in the present work, with the aim of reliably investigating on the influence of different parameters, a total scratching length of 100mm is reached for the testing of the sandstone material, and 20mm for the testing of granite samples.

Therefore, we designed a testing setup to study the forces during the cutting process, the tool penetration and the wear flat of the cutter by using a modified Cerchar abrasivity index (CAI) testing machine. The experimental setup, shown in Figure 2, comprises a CAI testing apparatus (i), based on the West [27] model, used to test the abrasiveness of the rock samples (ii). A linear actuator (iii) is implemented into the setup in order to precisely control the testing speed, scratching distance and also to measure the forces exerted on the scratching tool during the test. An inductive position sensor measures the vertical penetration of the scratching tool into the material (iv). The resulting wear flat at the tool's tip is optically imaged under a microscope with a magnification of 5-10X.

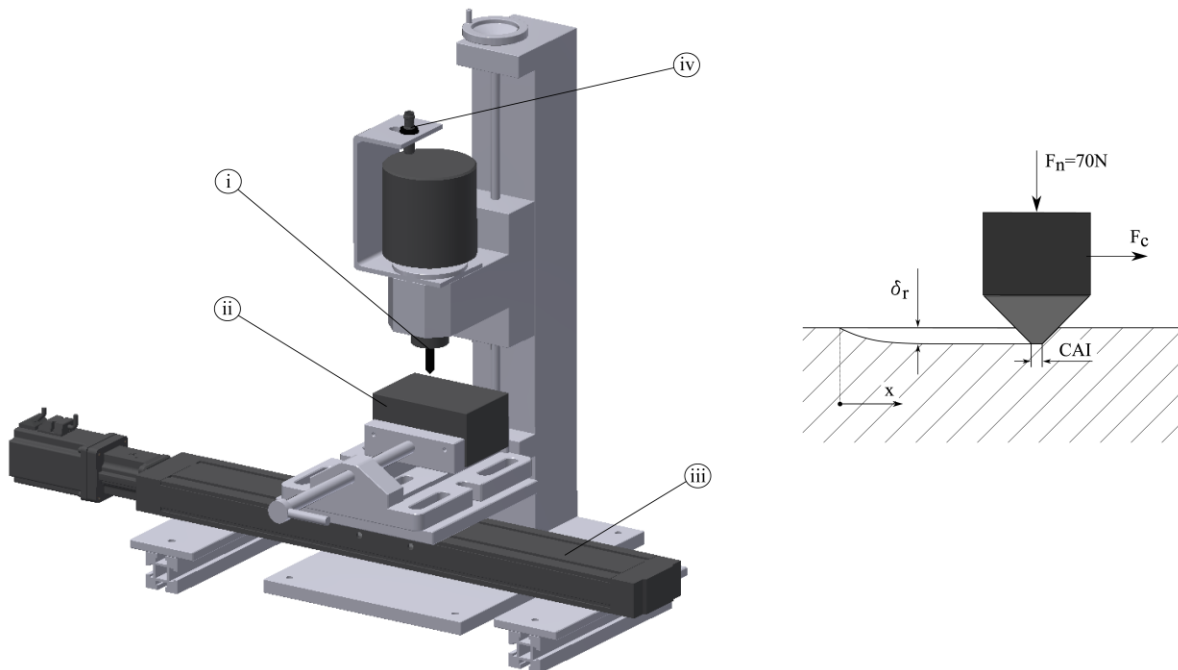


Figure 2: Experimental setup used to perform the experiments. The CAI tool (i) scratches the rock sample (ii), which is attached to a linear actuator (iii). A position sensor (iv) measures the vertical displacement of the scratching tool. On the right, the main parameters used in the rock-bit interaction: δ_r is the tool penetration, CAI the Cerchar abrasivity index, x is the scratching distance, F_n and F_c are the normal and cutting forces exerted on the tool during the test, respectively.

3.3 Thermal treatments

The combined thermo-mechanical drilling method is experimentally emulated by performing experiments on thermally treated samples. The thermal assistance to drilling, introduced in the proposed drilling method, is evaluated by testing the rock-bit interaction of oven-treated samples, compared to the baseline material. Therewith, rock samples are heat-treated in an inductive oven at a constant heating rate of $10^\circ\text{C}/\text{min}$, until the treatment temperature of 800°C is reached. This is held for 30 minutes in order to reach a homogeneous temperature inside the solid. After that, the samples are water-cooled with flushing water with the aim of reproducing the conditions found in a borehole during drilling with the proposed method. Samples are dried under laboratory conditions and tested at room conditions using the above-described experimental setup to compare the rock-bit interaction under baseline (untreated) and treated conditions.

4. RESULTS

In the following, the rock-bit interaction is investigated on granite and sandstone comparing the results under baseline conditions and after the thermal treatment. Cutting forces, tool penetration, exported rock and worn tool volume are finally employed to quantify the performance improvements of the proposed drilling method. The study also focuses on the specific mechanisms governing the rock removal by a sharp cutter.

The CAI before and after the thermal treatment gives insight on the resulting material abrasiveness and, by this, on the tool's wear flat reduction induced by the high temperature heating. The CAI value for the sandstone material is measured for increasing scratching length up to 100mm. Each test is conducted starting from sharpened tool conditions and three tests are carried out for each scratching distance value. This methodology allows to monitor the wear evolution at the tool's tip as the length of the scratch increases, or alternatively, during penetration of the tool into the sample's surface. The results for Rorschacher sandstone are shown in Figure 3.a. For small scratching distances below 5mm, a steep increase of CAI value is found for this material. After this, under baseline conditions, at a scratching distance of 10mm, the CAI reaches a value of 1.1 which corresponds to about 60% of the final value measured at a scratching distance of 100mm. This shows that, especially for the sandstone during baseline conditions, a testing distance above 20mm gives more representative results of the material abrasiveness [21, 28]. Sandstone samples, after oven-treating the material at 800°C and a water-cooling process, show decreased values of CAI (see Figure 3.a) over the entire range of tested scratching distance. This decrease of material abrasiveness after high-temperature thermal treatments is in agreement with the decline of mechanical properties reported after very high temperatures [29, 30] and fast cooling processes [31, 32]. For test distances below 20mm, we observe an overall 15-20% difference in CAI value, when baseline and treated conditions are compared. After this, the thermally-altered material shows a constant CAI value of about 1.1 until the maximum scratching distance of 90mm, whereas the baseline case follows a stable increase up to about 1.8. This discrepancy is a further indication of the thermally induced cracking of the material [15] and therewith the treated samples behave as low-abrasiveness materials, i.e. most of the abrasivity increase is found in the first 10mm of scratching distance. The measured data for baseline and thermally treated sandstone are fitted with a power law and a Langmuir absorption model, respectively, this is shown in Eq. (1).

$$CAI_{sandstone_base}(x) = 0.21 + 0.42 \cdot x^{0.30} \quad R^2 = 0.99 \quad (1.a)$$

$$CAI_{sandstone_800\ wc}(x) = \frac{1.19 \cdot 0.14 \cdot x^{1+0.41}}{1 + 0.14 \cdot x^{1+0.41}} \quad R^2 = 0.96 \quad (1.b)$$

where x is the scratching distance in [mm]. For the granite material, a testing distance of 100mm is not achievable, as the tool exhibits a strong sliding behavior which compromises the accuracy of the results for this scratching distance. Therefore, in the following, the data for granite is shown until a maximum scratching distance of 20mm. The results for the granite material are shown in Figure 3.b. Under baseline (untreated) conditions, granite samples have abrasiveness values around 3 to 4 times higher compared to the baseline sandstone material, this is also in agreement with literature data [33]. The granite material under baseline conditions shows a dramatic increase of CAI during the first 6mm of scratching distance. After this, the value increases only by 5% until the maximum scratching distance of 20mm. The treated granite, on the other hand, shows a less abrupt increase and, over the whole range of scratching distance, the CAI value is stably 50% lower, compared to the baseline material. The measured CAI value is interpolated over the scratching distance x using power functions, as in Eq. (2).

$$CAI_{granite_base}(x) = 0.75 + 2.11 \cdot x^{0.18} \quad R^2 = 0.99 \quad (2.a)$$

$$CAI_{granite_800\ wc}(x) = 0.06 + 1.19 \cdot x^{0.33} \quad R^2 = 0.95 \quad (2.b)$$

In order to test granite samples for larger scratching distances in a more reliable and consistent manner, an increase of the normal load on the tool would enhance the penetration of the tool during the experiment, also for very-abrasive materials. In this work, in order to preserve a certain consistency with the standard CAI test, this value was not varied from the standard 70N of normal force prescribed in [26].

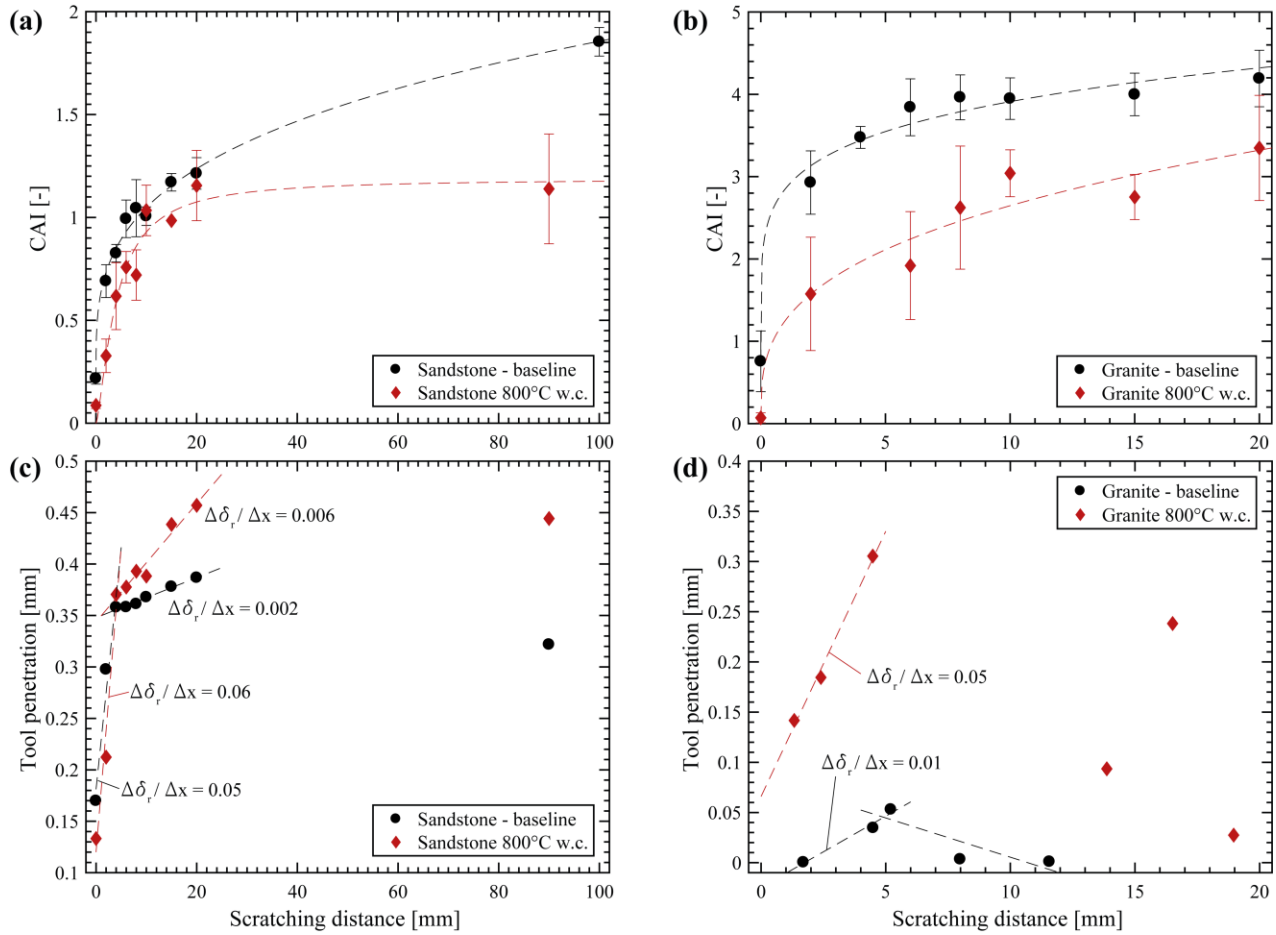


Figure 3: Cerchar abrasivity index values and the measured tool penetration along the scratching distance are shown for baseline and treated conditions for Rorschacher sandstone (a) and (c), and Central Aare granite (b) and (d).

The tool penetration during the CAI test is a representative measure for the removal performances of the proposed drilling method. The displacement sensor, located on top of the scratching tool, measures the total displacement of the tool into the rock material. This measure includes both the actual tool penetration, δ_r , and the worn height lost at the tool's tip during the CAI test, $h_t = \text{CAI}/2$. Therefore, from simple geometrical considerations, the actual tool penetration can be obtained using the measured CAI value at different scratching distances. The tool penetration for the baseline and treated conditions is shown in Figure 3.c and 3.d for sandstone and granite, respectively. As can be seen in Figure 3.c for sandstone, as the scratching distance increases in the range 0–4mm, the tool rapidly penetrates into the rock material until values of, namely, $\delta_r = 0.35\text{mm}$ for baseline and $\delta_r = 0.37\text{mm}$ for treated conditions, are reached. After this, the penetration continues to increase but at lower rates until the maximum penetration values are achieved. The peak penetration for the thermally treated sandstone, found at $x = 20\text{mm}$, is 20% higher, compared to the penetration into the baseline material. In this range, a linear regression of the penetration data over the scratching distance gives a 3-times-higher slope for the thermally treated material, compared to baseline conditions. Therewith, a tool penetration advance in the thermally treated sandstone requires a 3 times lower force increase, compared to the baseline material. When the scratch is extended until the maximum tested distance of $x = 90\text{mm}$, the baseline sandstone shows a slightly decreased penetration, compared to the value observed at $x = 20\text{mm}$. Whereas in the case of the thermally treated material, the penetration decrease at 90mm is less pronounced and the peak penetration remains constant around 0.45mm.

Therewith, we observe two distinct tool penetration behaviour as the scratching distance increases, for both the treated and baseline sandstone conditions. Firstly, the tool penetration rapidly increases for $0 < x < 4\text{mm}$, and both the baseline and treated conditions behave similarly. Afterwards, for scratching distances above 4mm, the tool penetration increase is less pronounced with increasing scratching distance. Further, in this second regime, the two material conditions – under baseline and after the thermal treatment – show significant differences as the scratching distance is further increased until 20mm. A comparison between the CAI results over the scratching distance (see Figure 3.a) and the resulting tool penetration (see Figure 3.c), suggests that the steep increase of tool penetration for small scratching distances, $0 < x < 4\text{mm}$, is coupled with a fast increase of CAI value and therefore a high rate of tool's wearing. The sharp transition between these two regimes appears at the same scratching distance of $x = 4\text{mm}$ for both the rock material conditions. As soon as a scratching distance above 4mm is reached, the tool penetration increase rate attenuates and this corresponds to a smaller increase of CAI value, i.e. a lower rate of tool's wearing over the scratching distance.

The tool penetration results for the granite material are shown in Figure 3.d. In this case, the tool initially penetrates the material, and, after a scratching distance of about 5mm, where the maximum penetration is found, the penetration starts to decrease until the maximum tested distance of 20mm. The baseline and the treated material similarly follow this trend. During baseline conditions, for small scratching distances, the penetration rate is low, compared to treated material conditions. At a scratching distance of 5mm, the maximum penetration of the tool $\delta_{r,max}=0.05\text{mm}$ is attained with a significant wearing of the tool (compare with Figure 3.b). Therefore, after this point, the tool penetration is impeded and the tool penetration drops to small values as the scratching distance increases. Concerning the thermally treated material, for scratching distances in the range $0 < x < 5\text{mm}$, the tool penetrates into the treated material with a high rate of $\Delta\delta_r/\Delta x=0.05$, which is five times higher than the corresponding penetration rate in the baseline granite. As soon as the maximum value of $\delta_{r,max}=0.3\text{mm}$ is reached, the tool penetration starts to decrease and slowly falls back to lower values. This phenomenon is evidently more visible in the granite material than the softer and less abrasive sandstone.

The cutting forces, exerted on the tool during the test, are fundamental in order to evaluate the improvements of the proposed drilling method in terms of the energy required to remove the material. The linear actuator continuously measures the cutting forces during the penetration of the tool into the sample material. These are shown in Figure 4.a and 4.b for sandstone and granite, respectively, under baseline conditions and after the thermal treatment. In the sandstone material (see Figure 4.a), for small tool penetration values $\delta_r < 0.35\text{mm}$ under baseline, and $\delta_r < 0.37\text{mm}$ for the treated material, the cutting forces are almost constant increasing tool penetration values. In this phase, the forces exerted to remove the thermally treated sandstone material are firmly 12% lower, compared to the baseline material. This small penetration regime corresponds to the first stage of tool's wearing (for $x < 4\text{mm}$), which was also observed in Figure 3.c regarding the tool penetration along the scratching length. For higher tool penetration values, above 0.35mm for the baseline material and 0.37 for the treated sandstone, the cutting forces follow an abrupt increase with the tool penetration until the peak penetration values are reached, namely, $\delta_{r,max}=0.38\text{mm}$ for baseline sandstone, and $\delta_{r,max}=0.46\text{mm}$ for the thermally treated material. The cutting forces quickly increase with the tool penetration in this stage, following a linear behaviour, as shown in Figure 4.a with the corresponding slopes. Here, the cutting tool requires an almost four times smaller force increase to advance in the penetration of the thermally treated material, compared to the baseline sandstone. The sharp transition between the first regime, exhibiting high tool's wearing and penetration with low required cutting forces, and a second regime, where the rate of tool's wearing is lower and higher cutting forces are measured, indicates that two different removal mechanisms are taking place as the tool penetration increases. In the first phase, the tool rapidly wears out and large penetration into the material are measured, until a threshold penetration is reached and, after this, the scratching process is governed by the compressive stresses developing in front of the cutting tool. In this second stage, low additional penetrations and tool's wear flat are attained with necessarily higher cutting forces.

The results concerning the cutting forces exerted on the tool during the removal of the granite material are shown in Figure 4.b. In the case of granite, the cutting forces stably increase as the tool penetrates into the material, both for baseline and for thermally treated material conditions. The required force increase to advance the tool penetration in the baseline granite is slightly higher, compared to the thermally treated material. Nevertheless, for the same applied cutting forces, a doubled tool penetration into the thermally treated material is found, compared to baseline conditions. Considering the force evolution with scratching distance, it can be observed that, as the tool removal proceeds in the untreated granite, a peak force value of 53N is reached for a penetration of $\delta_r=0.05\text{mm}$. This corresponds to the maximum achieved tool penetration and therewith the reversal point for the tool advance into the baseline material during the test (compare with Figure 3.d). A similar trend is observed for the thermally treated granite. In this case, the maximum penetration is about 0.3mm, a 6 times higher value compared to the baseline material, and the measured cutting force reaches a peak of 77N, after this, the tool penetration decreases and the cutting force drops until a value of almost 40N.

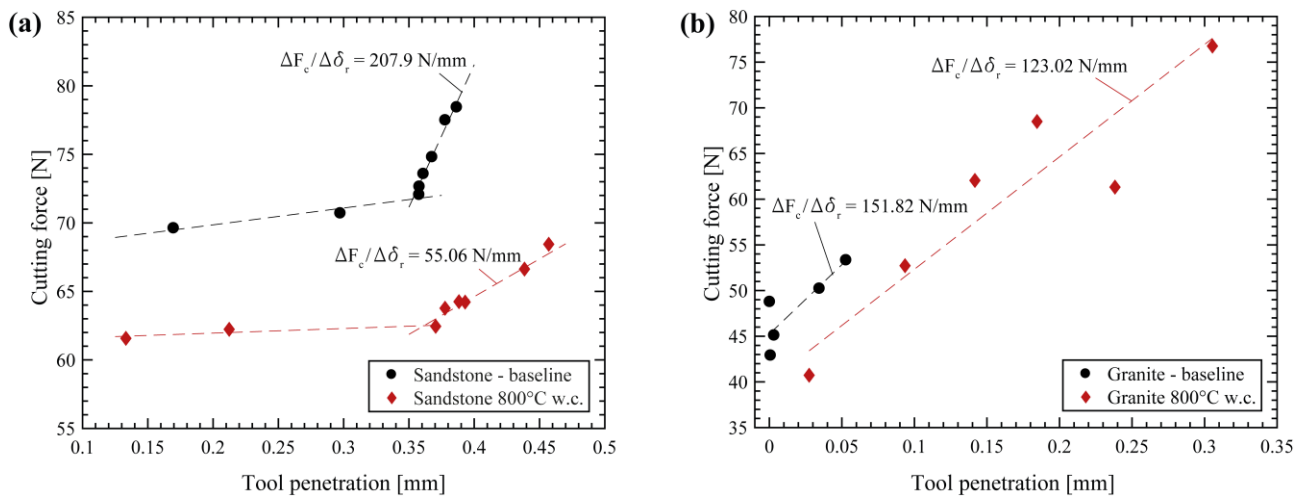


Figure 4: Cutting forces over the occurring tool penetration in the rock material for Rorschacher sandstone (a), and Central Aare granite (b) during baseline conditions and after the thermal treatment.

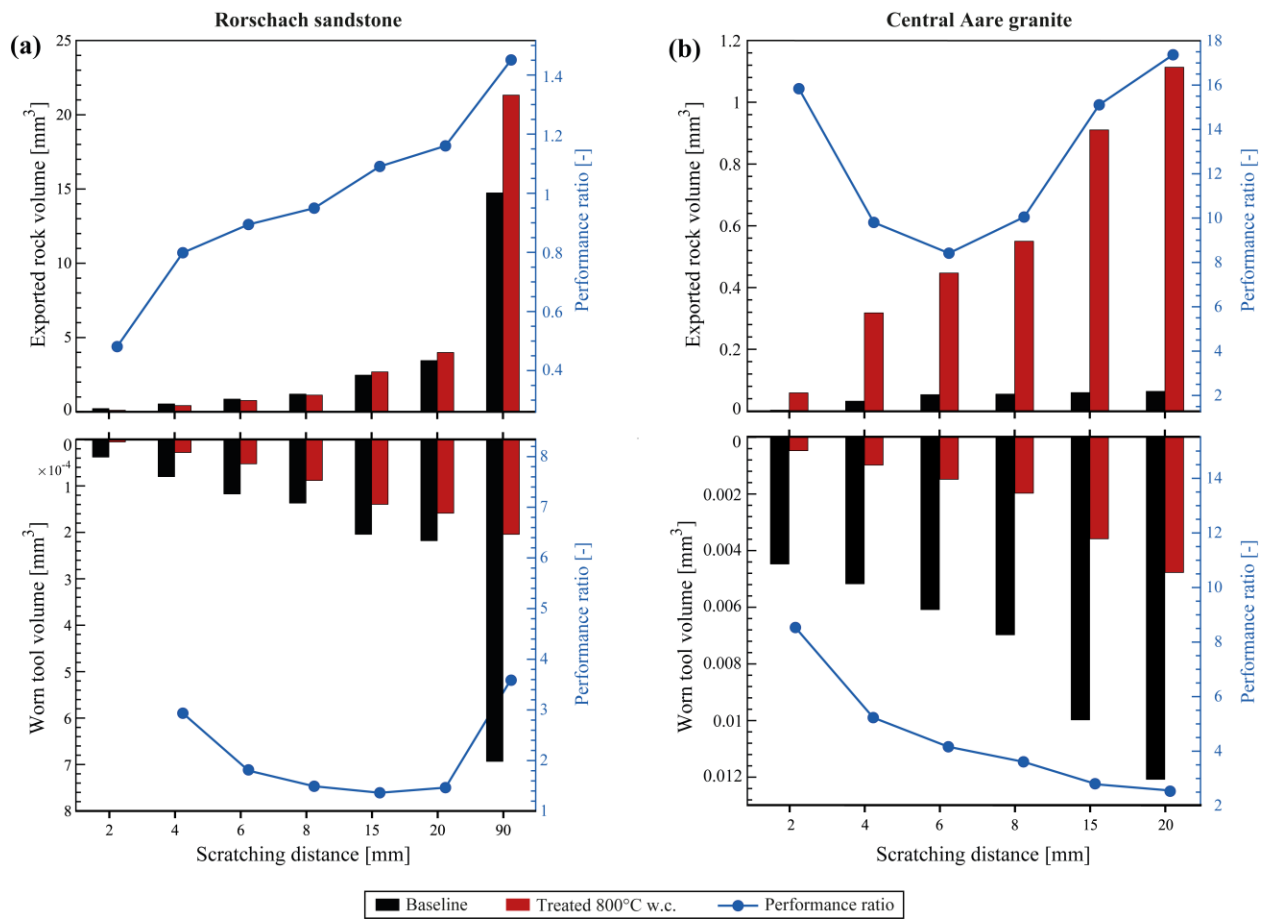


Figure 5: Cumulative volume of exported rock material and cumulative worn tool material at different scratching distances in Rorschacher sandstone (a) and Central Aare granite (b) during baseline and after the thermal treatment (bar plot, left axis). The performance ratio (blue curve, right axis) indicates the performance enhancement in terms of increased exported rock volume and reduced worn tool volume for the thermally treated rock material.

To summarize the rock removal enhancement and the tool’s wearing reduction of the proposed drilling method, we compare the volume of exported rock material and the worn volume at the tool’s tip during the test under baseline and thermally treated conditions, for both the materials. The knowledge of the tool penetration along the scratching distance, together with the CAI value, permit to quantify, from simple geometrical considerations, the cumulative exported rock volume and the cumulative volume of lost, worn material at the cutting tool. A performance ratio is defined to quantify the relative increase of exported rock volume and the reduction of tool’s wearing for the thermally treated material case, compared to baseline conditions, for both sandstone and granite. This is shown in Figure 5, where the performance ratio (blue curve) is plotted next to the absolute values (bar plot). In Figure 5.a, the results for the sandstone material are shown. For small scratching distances, $x < 20\text{mm}$, there is only a slight difference in the rock volume exported from the baseline and the thermally treated sandstone materials. However, in the same scratching distance range, the tool used to remove the thermally treated sandstone shows overall halved worn volumes (see bottom plot in Figure 5.a). As the scratching distance increases to 100mm, and the tool continues to penetrate the material, the superior drilling performances in the thermally treated material are indicated by a 40%-larger exported rock volume and by an almost 4 times smaller worn volume at the tool’s tip. This highlights the performance improvements which are achievable when a thermal assistance is implemented to enhance the mechanical drilling of sandstone, both in terms of increased exported rock material and reduced tool’s wearing. Further, this significant performance increase is attained with an almost 4 times lower force increase as the penetration advances, as previously discussed in Figure 4.a.

In Figure 5.b, we compare the cumulative volume of exported rock and worn tool material, for granite under baseline and thermally treated conditions. It can be promptly observed that there is one order of magnitude of difference in the volume of exported rock and worn tool material, when comparing the sandstone (Figure 5.a) and the granite (Figure 5.b). In this highly abrasive, hard rock material, the performance enhancement, achieved by thermally assisting the mechanical rock removal, are even more accentuated. As shown in Figure 5.b, during the removal of the thermally treated granite material for scratching distances below 8mm, the exported rock volume is overall one order of magnitude higher, compared to baseline conditions. Nevertheless, as the test is extended until a scratching length of $x = 20\text{mm}$, the cumulative removed rock volumes are 0.06 and 1.1 mm³, an almost 18 times larger exported rock volume is measured for the thermally treated granite material, compared to baseline conditions. From the bottom plot in the same figure, the volume lost at the tool’s tip is shown. Here, we observe a stable increase of worn tool volume over the scratching distance for both the material conditions and, for small scratching distances below 8mm, the worn tool material for the treated granite case is 4-to-9 times lower, compared to the baseline granite.

Finally, for the total scratching distance of 20mm, a performance ratio of 3 is found. Therefore, the drilling performance in thermally treated granite, shows overall 15-20 times larger exported rock volumes and 3-5 times lower rate of drill bit wearing.

5. CONCLUSION

We propose an alternative drilling method, called combined thermo-mechanical drilling, where conventional, mechanical drilling is thermally assisted to enhance the drilling performance in all types of rocks. In order to assess the performance of the combined thermo-mechanical drilling method, in this work, we analyze the rock-bit interaction of a sandstone and a granite material, comparing the baseline conditions with the material after a thermal treatment. For sandstone under baseline and thermally treated conditions, two distinct removal regimes are identified. A first phase, characterized by high rates of tool's wearing and steep tool penetration increases at low cutting forces, is found for low scratching distances. A second phase for larger scratching distances, where the tool's wearing and penetration are attenuated with required high cutting forces. In this second regime, the thermally treated material shows four times lower forces required to advance in the tool's penetration. This suggests that thermally treating the material allows to increase the penetration of the cutting tool with reduced drilling torque and therefore lower energy consumption. Furthermore, this method is capable to reduce the occurring drill bit wearing by almost a factor of 4 in the sandstone material, compared to conventional, rotary drilling methods. For the granite material, thermally treating the rock material can greatly improve the drilling performance of the drill bit, and namely, increasing by almost 15 times the removed rock volume and reducing the wearing of the drilling cutters by 3-to-5 times, compared to conventional drilling. These improvements are also attained with overall 20% lower forces at the drilling cutters and therefore at a lower energy input for the mechanical cutting of the rock material. Therefore, we conclude that the combined thermo-mechanical drilling method considerably enhances the drilling performance for geothermal resources by increasing the rates of penetration in both granite and sandstone. Additionally, the drilling costs are substantially diminished by improving the drill bit life and reducing the overall drilling time.

REFERENCES

1. Angelone, M. and S.S. Labini: Overcoming Research Challenges for Geothermal Energy. *Energy Research Knowledge Centre (ERKC), European Commission*. p. 36-36, (2014).
2. Uihlein, A. and B. Sigfusson: 2015 JRC Geothermal Energy Status Report. p. 60, (2015).
3. Tester, J.W., B. Anderson, A. Batchelor, D. Blackwell, R. DiPippo, E. Drake, J. Garnish, B. Livesay, M.C. Moore, and K. Nichols: The Future of Geothermal Energy. *Idaho National Laboratory*, (2006).
4. Glowka, D.A.: Design considerations for a hard-rock PDC drill bit. *Sandia report: Albuquerque, NM*. p. 23, (1985).
5. Fay, H. Practical Evaluation of Rock-Bit Wear During Drilling, in *SPE Drilling & Completion*. June 1993.
6. Teodoriu, C. Use of Downhole Mud-Driven Hammer for Geothermal Applications, in *37th Workshop on Geothermal Reservoir Engineering*. Stanford University, Stanford, California, January 30 -February 1, 2011.
7. Rudolf von Rohr, P., M.A. Kant, and E. Rossi: An apparatus for thermal spallation of a borehole, EP17188149.3, (2017).
8. Kant, M.A., E. Rossi, J. Duss, F. Amann, M.O. Saar, and P. Rudolf von Rohr: Demonstration of thermal borehole enlargement to facilitate controlled reservoir engineering for deep geothermal, oil or gas systems. *Applied Energy*, **212**, (2018).
9. Anders, E., F. Lehmann, and M. Voigt. Electric Impulse Technology-Long Run Drilling in Hard Rocks, in *ASME 2015 34th International Conference on Ocean, Offshore and Arctic Engineering OMAE2015*. St. John's, Newfoundland, Canada, May 31-June 5, 2015.
10. Timoshkin, I.V., J.W. Mackersie, and S.J. MacGregor. Plasma channel microhole drilling technology. *IEEE in 14th IEEE International Pulsed Power Conference*. Dallas, Texas, 15-18 June, 2003.
11. Hahn, S., M. Duda, F. Stoeckert, V. Wittig, and R. Bracke: Extended horizontal jet drilling for EGS applications in petrothermal environments. In: *EGU conference - geophysical research abstracts.*, **19**(EGU2017-14125), (2017).
12. Browning, J.A., W.B. Horton, and H.L. Hartman. Recent advances in flame jet working of minerals, in *7th Symposium on Rock Mechanics*. Pennsylvania State Univ, 1965.
13. Calaman, J. and H. Rolseth, Jet Piercing - Chapter 6.4, in *Surface Mining*. 1968: New York, USA. p. 325-337.
14. Kant, M.A., E. Rossi, C. Madonna, D. Höser, and P. Rudolf von Rohr: A theory on thermal spalling of rocks with a focus on thermal spallation drilling. *Journal of Geophysical Research: Solid Earth*, **122**(3): p. 1805-1815, (2017).
15. Rossi, E., M.A. Kant, F. Amann, M.O. Saar, and P. Rudolf von Rohr. The effects of flame-heating on rock strength: Towards a new drilling technology, in *51st Rock Mechanics/Geomechanics Symposium (ARMA)*. San Francisco, CA, USA, 25-28 June, 2017.
16. Schuler, M.: Fundamental Investigations of Supercritical Water Flows for Hydrothermal Spallation Drilling. *PhD Thesis no. 21803, ETH Zürich*, (2014).
17. Rothenfluh, T.: Heat transfer phenomena of supercritical water jets in hydrothermal spallation drilling. *PhD Thesis no. 21001, ETH Zürich*, (2013).
18. Stathopoulos, P.: Hydrothermal Spallation Drilling Experiments in a Novel High Pressure Pilot Plant. *PhD Thesis no. 21163, ETH Zürich*, (2013).

19. Kant, M.A., E. Rossi, D. Becker, and P. Rudolf von Rohr. Enhancing the Drilling Process for Geothermal Resources by Combining Conventional Drilling and the Spallation Technology in *42nd Workshop on Geothermal Reservoir Engineering*. Stanford University, Stanford, California, February 13-15, 2017. SGP-TR-212, 2017.
20. Kant, M.A., J. Ammann, E. Rossi, C. Madonna, D. Höser, and P. Rudolf von Rohr: Thermal properties of Central Aare granite for temperatures up to 500°C : irreversible changes due to thermal crack formation. *Geophysical Research Letters*, **44**, (2017).
21. Hamzaban, M.T., H. Memarian, and J. Rostami: Continuous monitoring of pin tip wear and penetration into rock surface using a new cerchar abrasivity testing device. *Rock Mechanics and Rock Engineering*, **47**(2): p. 689-701, (2014).
22. Capik, M. and A.O. Yilmaz: Correlation between Cerchar abrasivity index, rock properties, and drill bit lifetime. *Arabian Journal of Geosciences*, **10**(1), (2017).
23. Plinninger, R.J. and K. Thuro. Wear Prediction in Hardrock Excavation Using the CERCHAR Abrasiveness Index (CAI), in *EUROCK 2004 & 53rd Geomechanics Colloquium*. Salzburg, Austria, 6-8 October, 2004.
24. Alber, M.: Stress dependency of the Cerchar abrasivity index (CAI) and its effects on wear of selected rock cutting tools. *Tunnelling and Underground Space Technology*, **23**(4): p. 351-359, (2008).
25. Cerchar: Centre d'Etudes et Recherches des Charbonnages de France. The CERCHAR abrasiveness index. *Verneuil 12S*, (1986).
26. ASTM: Standard Test Method for Laboratory Determination of Abrasiveness of Rock Using the CERCHAR Method. *ASTM International*. p. 1-6, (2010).
27. West, G.: Rock abrasiveness testing for tunnelling. *International Journal of Rock Mechanics and Mining Sciences and Geomechanics Abstracts*, **26**(2): p. 151-160, (1989).
28. Rostami, J., A. Ghasemi, and F. Dahl: Study of Dominant Factors Affecting Cerchar Abrasivity Index. *Rock Mechanics and Rock Engineering*, **47**: p. 1905-1919, (2014).
29. Hajpál, M. and Á. Török: Mineralogical and colour changes of quartz sandstones by heat. *Environmental Geology*, **46**: p. 311-322, (2004).
30. Ranjith, P.G., D.R. Viete, B.J. Chen, and M.S.A. Perera: Transformation plasticity and the effect of temperature on the mechanical behaviour of Hawkesbury sandstone at atmospheric pressure. *Engineering Geology*, **151**: p. 120-127, (2012).
31. Brotóns, V., R. Tomás, S. Ivorra, and J.C. Alarcón: Temperature influence on the physical and mechanical properties of a porous rock: San Julian's calcarenite. *Engineering Geology*, **167**: p. 117-127, (2013).
32. Shao, S., P.L.P. Wasantha, P.G. Ranjith, and B.K. Chen: Effect of cooling rate on the mechanical behavior of heated Strathbogie granite with different grain sizes. *International Journal of Rock Mechanics and Mining Sciences*, **70**: p. 381-387, (2014).
33. Thuro, K. and G. Spaun: Testing conditions and geomechanical properties influencing the CERCHAR abrasiveness index (CAI) value. *International Journal of Rock Mechanics and Mining Sciences*, **40**: p. 259-263, (2003).